



# Structural modeling and simulation studies of *Brugia malayi* glutathione-S-transferase with compounds exhibiting antifilarial activity: Implications in drug targeting and designing

Marshleen Yadav<sup>a</sup>, Alka Singh<sup>a</sup>, Sushma Rathaur<sup>a,\*</sup>, Eva Liebau<sup>b</sup>

<sup>a</sup> Department of Biochemistry, Faculty of Science, Banaras Hindu University, Varanasi 221005, U.P., India

<sup>b</sup> Westfälische Wilhelms-Universität, Institute of Animal Physiology, Department of Molecular Physiology, Hindenburgplatz-55, Muenster, Germany

## ARTICLE INFO

### Article history:

Received 8 July 2009

Received in revised form 27 September 2009

Accepted 18 October 2009

Available online 31 October 2009

### Keywords:

Glutathione-S-transferase

Antifilarials

Chalcones

Homology Modeling

Docking

## ABSTRACT

Since glutathione-S-transferase (GST) mediated xenobiotic detoxification is a crucial mechanism in nematodes survival, we aimed to conduct an *in silico* analysis of filarial GST in order to predict the possible interactions for antifilarials. Present report depicts the homology modeling approach applied in the construction of molecular structure of *Brugia malayi* GST (BmGST) followed by its docking simulation with available antifilarials such as diethylcarbamazine, albendazole, Butylated Hydroxyanisole (BHA) and substituted chalcones. A very low root mean square deviation (0.82 Å) from template structure and stereochemical quality of constructed BmGST model proposed it as a significant framework for further analysis. In docking studies antifilarials and chalcones exhibited demarcation in their binding affinity and modes. Amongst all the compounds studied, albendazole and methyl-substituted chalcone showed the lowest binding energy and occupied binding pocket near to substrate binding site of GST. The side chain of these compounds interplayed as a potential interaction site which targeted mainly hydrophilic residues of the BmGST. The structural information and binding site mapping of BmGST for different antifilarials obtained from this study could aid in screening and designing new antifilarials or selective inhibitors for chemotherapy against filariasis.

© 2009 Elsevier Inc. All rights reserved.

## 1. Introduction

Glutathione-S-transferases are major phase II detoxification enzymes in parasitic system. Because of their detoxifying nature [1] and maintenance of cellular redox status [2] they are widely used in drug inhibition studies and have become tempting drug targets in various helminth diseases [3–5]. GSTs catalyze the conjugation of glutathione with various endogenous and exogenous xenobiotics substrates for degradation in form of inactivation and excretion [6–8]. The multifunctional roles [9] and comparatively high cellular levels of GSTs strongly signify their role in drug resistance as they are found to be inducible during drug intake [10]. In parasitic context their role can be elaborated by the fact that some of these organisms lack the cytochrome P450 system, a phase I detoxification enzyme [11].

In our earlier reports we have shown the induction of filarial GST from *Setaria cervi* by diethylcarbamazine (DEC, known

antifilarial) and a prototypic inducible compound Butylated Hydroxyanisole (BHA) [12], whereas, our recent communication establishes the inhibition of *S. cervi* GST (ScGST) activity by substituted chalcones and proposed them as antifilarials [13]. These studies were undertaken in *in vitro* conditions to observe the effect of aforementioned compounds on parasite survival and GST activity. In order to understand the interaction of antifilarials with parasite GST at atomic level we have performed homology modeling of GST from *Brugia malayi* (BmGST) followed by its docking studies with antifilarials compounds. The information of predicted binding map of BmGST from this study would aid in structural analysis and screening and designing new antifilarials for future aspects since continuous administrations of existing drugs can raise the possibility of resistance in parasites.

## 2. Materials and methods

### 2.1. Protein homology modeling

The modeling assignment was done on SWISS-MODEL [14] ([www.swissmodel.expasy.org/SWISS-MODEL.html](http://www.swissmodel.expasy.org/SWISS-MODEL.html)). Protein

\* Corresponding author. Tel.: +91 542 2307323; fax: +91 542 2368174.  
E-mail addresses: [surathaur@rediffmail.com](mailto:surathaur@rediffmail.com), [sushmarathaur@yahoo.com](mailto:sushmarathaur@yahoo.com) (S. Rathaur).

sequence of *Brugia malayi* GST (208 amino acid) was obtained from NCBI protein database (acc. no. XP\_001898233) and uploaded in fasta format on Swiss server. To obtain the closest match BLAST of query protein sequence was performed which searched against Protein Data Bank (ExPDB). Before sequence alignment hetero groups were removed from the template structure and raw sequence of target was refined. Structural alignment of target-template was done using ProModII program of Swiss server which first assigned the simple backbone for target sequence [15]. The optimization of other parameters such as addition of blocking groups, missing side chains, Polar H and loops were also operated on the same server.

## 2.2. Structure validation

After the construction of model, its quality was assessed on the basis of both geometric and energetic aspects. The structure was evaluated by ANOLEA force field, GROMOS 96 [16,17] and ERRAT ([www.doe-mbi.ucla.edu/Services/ERRAT/](http://www.doe-mbi.ucla.edu/Services/ERRAT/)). These tools provided the graphical presentation of energy minimization of obtained protein model. The stereochemical property was checked using PROCHECK. The Ramachandran plot provided the residue position in particular segments based on  $\varphi$  and  $\psi$  angles between N–C $_{\alpha}$  and C $_{\alpha}$ –C atoms of residue. Validated structure was then submitted to Protein Model Database (PMDb) as a homology model (PM0075818).

## 2.3. Ligand structure

For docking, the ligand (compounds) structures were prepared on Marvin sketch 5.0.7. The two dimensional structures of ligands were first added with explicit H and then cleaned in 3D environment using gradient optimization method. The obtained structures were run for molecular dynamics to see the flexibility of atoms. Simulation was performed in 1000 cycles using dreiding force field at 300 K. The best conformer thus obtained was based on energy minimization and geometry optimization. The final structures exhibiting lowest energy were saved in \*.pdb format to input in to Hex environment. The hydrophobicity (log *P*) of compounds was calculated by the method of Viswanadhan et al. [18].

## 2.4. Molecular docking

For docking process the entire protein structure was subjected on to Hex 5.1 at its default parameters with grid dimension of 1 Å for ligand docking without imposing any binding site. Hex is a tool for macromolecule docking and it can superpose pairs of molecules using only knowledge of their 3D shapes. Further, it is one of the few docking tools having in built graphic viewer [19,20]. This tool has been used in some earlier studies demonstrating ligand protein interaction [21,22]. The approach was to use blind docking since it has been recommended for acquiring good results in substrate binding site prediction [23]. Correlation type and post-processing output for receptor and ligand were kept based on shape, electrostatic potential and molecular mechanics (MM) minimization. Docking was carried out at full rotation allowing full flexibility for the ligand while keeping receptor position fixed in space as described earlier [24]. Docking parameters involved Fourier transformation, steric scan, final search for ligand binding site and refinement of the complex. The cluster solutions were based on energy with RMS value of 2.5 Å. For comparison purpose binding sites of ligand on protein receptor were also predicted by POCKET-FINDER tool which is based on POCKET algorithm and measures through a sphere of 3 Å with 3D grid line in x, y and z directions

and identify extent to which each grid point is buried in the protein [25].

## 2.5. Pose validation and evaluation

Docked poses were evaluated based on total energy and pose with lowest energy was saved in \*.pdb format. The interaction energy was calculated by following equation:

$$\Delta E_{total} = \Delta E + \Delta E_{ele}$$

where  $\Delta E_{vdw}$  and  $\Delta E_{ele}$  represent non-bonded van der Waals and electrostatic interaction between the substrate and each residue, respectively. The obtained conformations were inspected visually on Molecular Virtual Viewer 1.2.0 (Molegro) and Discovery studio 2.0 to analyze the type of interaction between ligand and protein. To identify the residues located in binding pocket, protein structure was truncated to 10 Å around the bound ligand. At this scale possible interaction (H-bonding, electrostatic, covalent and van der Waals) between residues and ligand were measured and highlighted.

## 3. Results and discussion

The BLAST result of BmGST showed 79.8% sequence similarity with a subunit of *Onchocerca volvulus* GST2 (OvGST2) [26] (1tu7B) suggested 1tu7B as a most suitable template for homology modeling (Fig. 1). Since *B. malayi* and *O. volvulus* belong to same family, i.e. Onchocercidae one can speculate high sequence similarity between the two. The structure was constructed on automated mode of SWISS-MODEL workspace with its default parameters. The root mean square deviation (RMSD) of obtained model was calculated by structural superposition of model and template (resolution 1.5 Å) on YASARA and was found to be 0.820 Å with E value of  $7.90 \times 10^{-96}$  which reflects a high structural homology between the two proteins. The total energy of BmGST model calculated by GROMOS96 force field was  $-45727.039$  kcal/mol which was further minimized up to  $-48011.697$  kcal/mol in 100 cycles on MOIL. The final refined conformer was validated by Ramachandran Plot which showed 170 residues (91.39%) in most favored region with 14 (8.59%) residues in generously allowed regions (Fig. 2A). This result is comparable to an earlier report where WbGST has been shown to display 93.5% residues in most favored region [24]. The quality of BmGST model was also confirmed by ERRAT which depicted a significant 96.5% quality factor for the structure (data not shown). The topological examination of this model exhibited a similar pattern of  $\alpha/\beta$  in whole protein stretched as found in 1tu7B and WbGST with four  $\beta$  turns and three  $\alpha$  helices towards N-terminal region forming domain I ( $\beta\alpha\beta\alpha\beta\alpha$  motif) while at C-terminal the five  $\alpha$  helices exclusively occupied the whole structure (domain II) defining its  $\pi$  class attribute [27] (Fig. 2B). The domains I and II form G-site (GSH binding site) and H-site (xenobiotic binding site), respectively [28] specifically for detoxification purpose. The arrangement of  $\alpha/\beta$  in both domains in such a manner reflects the structural conservation between species which might be due to the execution of similar functions. The overall frequency of different structural patterns detected in BmGST by PyMOL 1.0 [29] were 54.8% helix, 9.6% sheet, 13% turn, 19.2% coil and 3.4% 3–10 helix which is in accordance with an earlier report [30]. Electrostatic analysis of BmGST demonstrated a high electropositive surface apparently more towards the domain I. However, the ligand binding sites and top region of domain II were dominated by electronegative surface (Fig. 2C). Amino acid distribution pattern in BmGST suggested the occurrence of high amount of hydrophilic residues (located at the surface) compared to hydrophobic residues (buried inside the structure) reflect the solvent accessibility of structure



**Fig. 1.** BLAST sequence alignment of BmGST and 1tu7B using user-defined parameters of gap open and extension penalties with BLOSUM62 matrix. The highly aligned regions (\*) are shown in gray color.

(Supplementary material). A comparative study of amino distribution pattern in BmGST and human GST was also carried out which implicated that Tyr, Phe, Asp, Lys, His and Ile were significantly high in BmGST while other residues were either low or comparable to human GST (Fig. 3). Amongst above mentioned residues, Tyr, Asp and Lys play a crucial role in substrate binding and GST dimerization in parasites. In respect to structural evaluation 13 salt bridges were also detected between Asp, Lys, Glu, Arg and His in BmGST model using GRASP2. Amongst these residues, Asp and Arg alone contributed 4 salt bridges. It is reported that salt bridging between abovementioned residues keeps the enzyme in its native form which is generally required for catalytic mechanism [31].

Table 1 summarizes the chemical properties of compounds used in docking experiments. The log *P* value of all compounds was found to be less than 5 which defines their lipophilic nature and qualify these compounds for proper absorption and permeation in host body [32]. Amongst all compounds DEC showed lowest log *P* value demonstrating its potential as a drug in field application. However, the methyl-substituted chalcones (SK4, SK6 and SK7) also exhibited the comparable log *P* value proposing that these compounds could be as effective as DEC in absorption. The variation in solvent accessible surface (van der Waals) between antifilarials and chalcones could easily be observed and suggests that chalcone because of their bigger structure would bind towards proximal areas of protein receptor. The clustering of docked solutions varies for different drugs ranging from 106 to 323 (Table 2). The docked complexes were further optimized and minimized on MVV keeping protein structure fix in space.

Tables 3 and 4 depict the interaction of various compounds with BmGST. The interaction energy of each compound was calculated by ligand energy inspector menu of MVV. Residues located within 10 Å distance from ligand were considered as binding pocket. These pockets were however different from those detected by POCKET-FINDER (data not shown) except for

albendazole and methyl-substituted chalcones which occupied in one of the pocket buried between α 6 and α 8, site detected by above program. Except albendazole, BHA, SK4 and SK5 the rest of the compounds failed to form H-bond with protein receptor. Few residues such as Cys168 and Lys171 were common in binding pocket of BHA and chloro-substituted chalcones while Ile163 interplayed as a common binding residue for albendazole and methyl-substituted chalcones. However, interaction of DEC was noticeably different from other compounds and occupied a surface position towards the bottom of α helix of domain II.

### 3.1. Binding pocket of DEC

The binding site of DEC consisted of hydrophilic aliphatic side chain amino acid such as Glu129, Lys130, Asp137 and hydrophobic Leu174 (Table 3) of which Glu129 neighbors the Lys127, a participating residue in BmGST dimer formation [26]. Moreover, Glu129 interacted with lowest binding energy as shown in Table 4 while other residues did not exhibit comparable interaction with DEC but involved in proper anchoring of ligand. There were lack of H-bond, electrostatic and covalent sharing between DEC and binding residues despite of the presence of hydrophilic pocket as shown in Fig. 4Aa. The steric clashes between the DEC atoms and residues were significantly high which might be a reason for no interaction and promoted it to bind at the extreme surface site located far end of domain II α5 helix. The average distance between the ligand and residues was 4 Å which exceeds the optimal distance to form H-bond. The non-bonded interaction between DEC and amino acids were further supported by the analysis of interaction between nearby residues. As observed between Leu174:Glu129 and Ala126:Lys130 the H-bonding in undock structure remained intact even after the complex formation. This type of interaction could also be explained by a very low electrostatic potential in docking of DEC in BmGST as shown in Table 3.

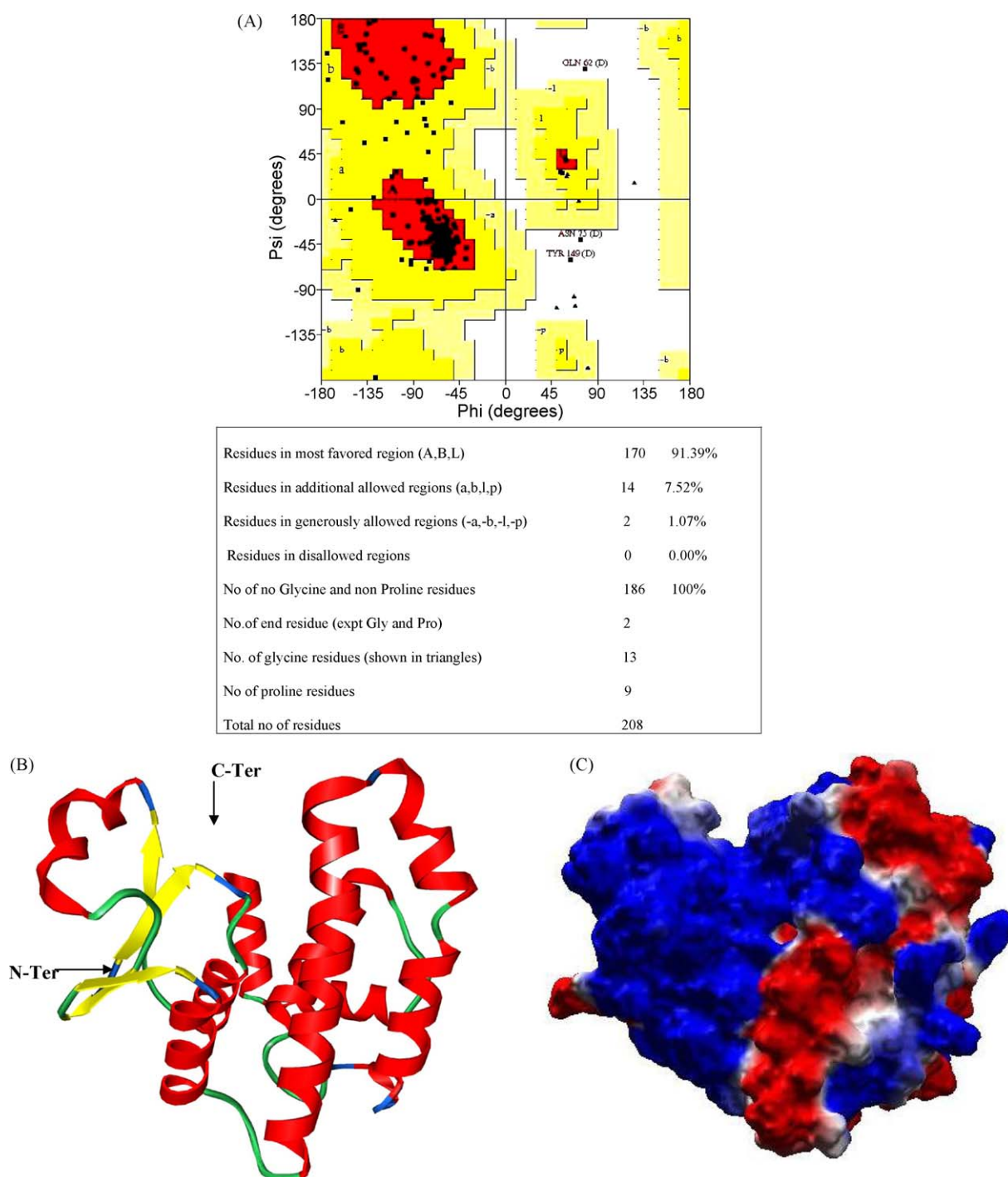


**Fig. 2.** (A) Ramachandran plot of BmGST. (B) Schematic representation of secondary structure of BmGST. Red regions:  $\alpha$ -helices, yellow color:  $\beta$  turns and blue and green regions: coils. Domains are highlighted by arrows. (C) Electrostatic surface of BmGST. Blue: electropositive regions and red: electronegative regions. Potential less than  $-10$  kT neutral and greater than  $10$  kT is displayed in red, white, and blue. (Figure produced using MVV 1.2.0; Molegro.)

### 3.2. Binding pocket of albendazole

Albendazole pocket was located between triangular surface of  $\alpha 1$ ,  $\alpha 6$  and  $\alpha 8$  formed by hydrophilic residues Arg11, Asp159, His179, Glu183, Arg195, Asn196 and a hydrophobic residue Ile at 163 and 200 position (Fig. 4Ab). In ligand docking Arg and Asn participated with lowest binding energy and formed 6 H-bonds with Alb (Tables 3 and 4) thus follow a recent report where Arg and Asn are shown as major H-bonding residues in binding pockets for organic compounds [33]. Oxygen (12) of Alb and NH1 of Arg11

were major atoms participated in formation of H-bonds. From depth analysis we found that O (12) from carbamate moiety of Alb was the most favorable interacting site since this atom alone made 4 H-bonds and exhibited lowest interaction energy ( $-55.053$  kcal/mol) while thiol and benzimidazole moiety of albendazole were anchored by electronegative residues such as Asp159, Glu162, His179 and Glu183. Arg 11 is situated at the opposite side and close to Tyr7 and Leu13 (GSH binding site) hence binding of albendazole at this position could lead to conformational changes in protein or causing steric hindrance which might interfere in GSH binding and



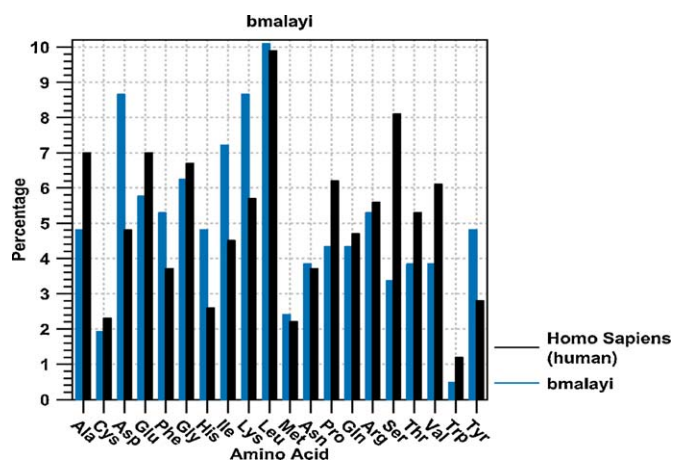


**Fig. 3.** Amino acid distribution histogram of BmGST compared to human GST. Blue bars; BmGST, Black bars; Human GST.

catalytic activity of GST. To conform it, we performed GSH docking in the presence of albendazole which showed that GSH indeed could not bind at Tyr7 (original binding site) and rather occupied position at outer surface of domain II. This dislocation of GSH in the presence of Alb suggests the inhibitory effect of Alb on GST activity.

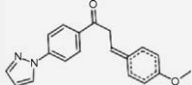
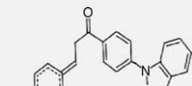
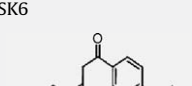
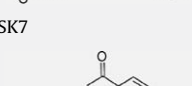
### 3.3. Binding pocket of BHA

The binding pocket of BHA consisted of equal number of hydrophilic and hydrophobic residues. Unlike DEC and albendazole, BHA accommodated between two  $\alpha$  helices ( $\alpha 5$  and  $\alpha 7$ ) noticeably buried inside the highly electronegative cavity consisted of Asp165, His167 and Asp170 with protrusion of its butyl moiety outside. Cys168 was found to be closest to BHA within a distance of 5 Å and formed one H-bond with hydroxyl group (O17) of BHA (Table 4). While a second H-bond was also formed between same atom of BHA (O17) and nitrogen atom of

**Table 1**  
Chemical properties of compounds used in docking study.

Compound	Molecular weight	Conformer energy (kcal/mol)	log $P^a$	van der Waals surface (Å)
DEC	199.168	29.0	2.26	374.14
ALB	265.088	59.66	3.47	375.93
BHA	180.115	40.02	3.14	319.64
SK1	308.084	68.82	3.94	418.14
SK2	309.079	66.47	3.58	409.71
SK3	326.131	69.02	4.61	479.83

**Table 1** (Continued)

Compound	Molecular weight	Conformer energy (kcal/mol)	log <i>P</i> <sup>a</sup>	van der Waals surface (Å)
SK4	305.129	72.09	2.81	440.28
				
SK5	356.139	85.74	3.67	495.07
				
SK6	324.159	75.26	2.78	496.05
				
SK7	306.149	68.24	2.95	465.77
				

<sup>a</sup> log *P*: hydrophobicity measurement.**Table 2**

Docking results of different compounds with BmGST.

Compound	Total cluster	$\Delta E_{total}$ (kcal/mol)	$\Delta E_{vdw}$ (kcal/mol)	$\Delta E_{ele}$ (kcal/mol)
DEC	290	−224.1	−183.5	40.60
ALB	175	−264.0	−237.2	−26.7
BHA	106	−213.2	−221.1	7.90
SK1	189	−288.5	−311.3	22.8
SK2	188	−287.4	−309.7	22.3
SK3	209	−289.2	−314.8	25.5
SK4	252	−258.2	−250.9	−7.30
SK5	323	−320.4	−350.5	30.0
SK6	229	−309.1	−309.4	0.30
SK7	239	−322.1	−320.1	−2.00

 $\Delta E_{total}$ : total binding energy;  $\Delta E_{ele}$ : electrostatic interaction energy;  $\Delta E_{vdw}$ : van der Waals interaction energy.**Table 3**

Binding energy of major residues involved in ligand docking.

Residues	$E_{total}$ (kcal/mol)	MolDock score <sup>a</sup>
DEC		−51.087
Glu129	−77.79	
Lys130	−28.11	
Asp137	−7.31	
Leu174	−46.88	
ALB		−70.662
Arg11	−48.88	
Arg195	−32.22	
Asn196	−21.36	
BHA		−58.078
Pro122	−27.89	
Asp165	−26.83	
His167	−44.86	
Cys168	−34.01	
Lys171	−8.835	
SK1		−77.756
Asp165	−80.91	
His167	−40.92	
Cys168	−34.57	
Lys171	−50.47	
SK2		−77.475
Asp165	−80.88	

**Table 3** (Continued)

Residues	$E_{total}$ (kcal/mol)	MolDock score <sup>a</sup>
His167	−41.10	
Cys168	−34.43	
Lys171	−48.82	
SK3		−77.076
Pro122	−52.23	
Cys168	−41.21	
Lys171	−64.99	
Phe172	−65.52	
SK4		−79.514
Gln162	−59.66	
Ile163	−97.24	
Pro166	−43.87	
Gln208	−86.49	
SK5		−87.934
Arg11	−32.17	
Gln162	−68.35	
Ile163	−54.43	
Asn196	−37.05	
SK6		−88.796
Asp159	−57.04	
Ile163	−37.09	
SK7		−96.967
Asp159	−47.06	
Ile163	−57.58	
Glu183	−64.13	

<sup>a</sup> MolDock score calculated by summing the external ligand interaction (protein–ligand interaction) and internal ligand interaction score using Virtual Molecular Viewer 1.2.0.

Pro122 located at a distance of 3.6 Å. The hydroxyl group of BHA acted as both donor and acceptor in these interaction due to its high interaction energy (−33.82 kcal/mol) and hydrophilic nature. The primary interaction appeared to be H-bond and van der Waals (Fig. 4Ac). However, C9 atom of BHA also exhibited the possibility of covalent bonding (0.802 kcal/mol) with its nearest residue Asp165. Besides interaction with above residues, docking of BHA also dissipated H-bonding between Asp165:Cys168 and His167:Asp170 (data not shown) leading to

**Table 4**

H-bond interaction between residues and compounds.

Compound	Residues forming H-bond	Distance (Å)	Bonding energy (kcal/mol)
<i>ALB</i>			
N (6) <sup>a</sup>	NH1 (115) Arg11 <sup>d</sup>	3.41	−4.04
O (12) <sup>a</sup>	NH1 (115) Arg11 <sup>d</sup>	2.87	−10.5
O (17) <sup>a</sup>	NH1 (115) Arg11 <sup>d</sup>	3.58	−1.61
O (12) <sup>a</sup>	NE (1948) Arg195 <sup>d</sup>	2.86	−8.56
O (12) <sup>a</sup>	NH2 (1951) Arg195 <sup>d</sup>	3.36	−2.61
O (12) <sup>a</sup>	ND2 (1965) Asn196 <sup>d</sup>	3.21	−4.12
<i>BHA</i>			
O (17) <sup>a,d</sup>	N (1208) Pro122 <sup>a</sup>	3.60	−1.66
O (17) <sup>a,d</sup>	O (1660) Cys168 <sup>a</sup>	3.35	−0.63
<i>SK4</i>			
N (3) <sup>a</sup>	N (2074) Gln208 <sup>d</sup>	3.29	−3.69
<i>SK5</i>			
O (25) <sup>a</sup>	NH1 (115) Arg11 <sup>d</sup>	2.94	−10.5
O (25) <sup>a</sup>	N (1965) Asn196 <sup>d</sup>	3.19	−8.66

<sup>a</sup>: acceptor, <sup>d</sup>: donor and <sup>a,d</sup>: both.

the conformational changes in protein and thus providing the possibility of alteration in biological activity of BmGST by BHA. In our earlier studies we have shown that BHA increases the GST activity 2 times compared to control [12]. Here, in depth analysis of the active site conformation after docking with BHA we observed that H-bond distance between thiol group of GSH and OH group of Tyr7 decreases to 2.962 Å as compared to 3.129 Å in control (Supplementary material). Hence, increase in GST activity could be either due to formation of stable complex between GSH and enzyme or change in the conformation of enzyme which increases the affinity for the second substrate.

### 3.4. Binding pocket of chalcones

Chalcones occupied two different binding locations depending upon their side group substitution and exhibited lowest binding energy and docking score compared to antifilarial drugs (Fig. 4Ba–Bg). A clear demarcation in binding efficiency was observed between chloro and methyl-substituted chalcones which reached to maximum in case of SK7 and comparable to our earlier

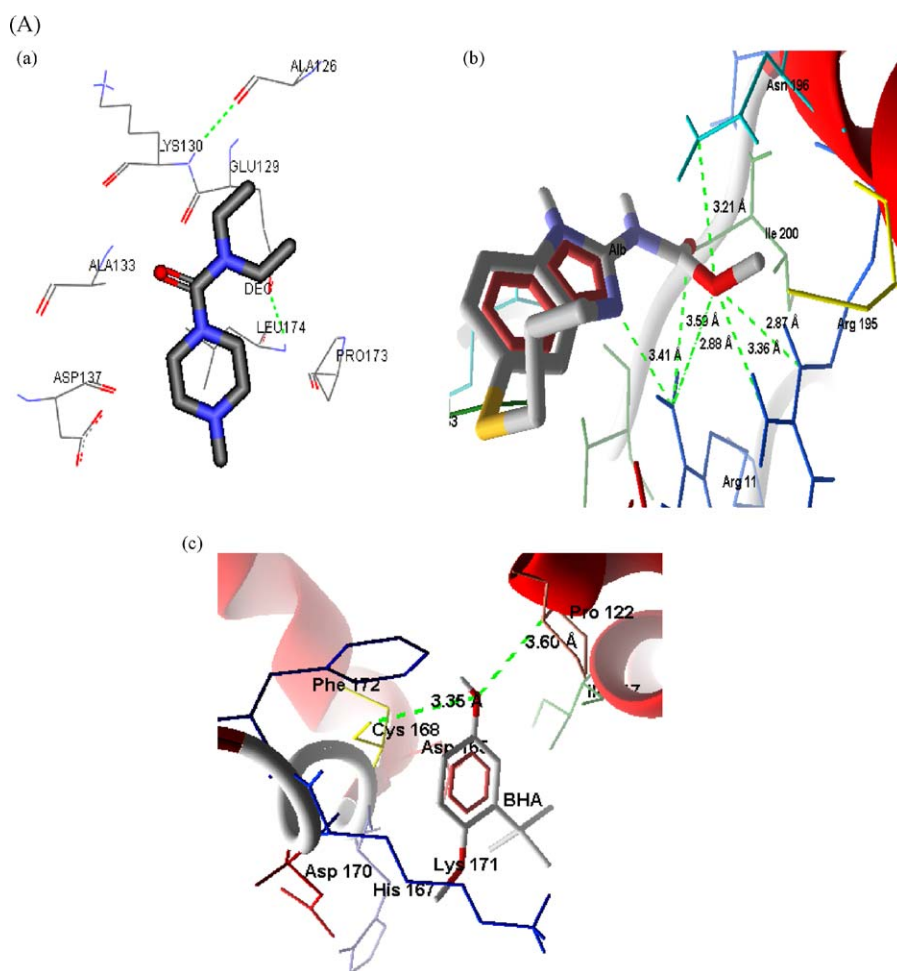


**Fig. 4.** (A) Predicted binding modes of antifilarials in BmGST. Best docked poses are represented in figures (a) diethylcarbamazine, (b) albendazole and (c) Butylated Hydroxyanisole. Residues and ligands are shown in wireframe and stick form respectively. Colored according to the atoms—gray: carbon, red: oxygen and blue: nitrogen. For clarity purpose hydrogen is omitted in ligands. Predicted hydrogen bonds between residues and ligand are highlighted with green dash lines and residues are colored according to amino acid type. Binding site represented with ribbon structure (red) wherever required. (B) Predicted binding modes of chloro and methyl-substituted chalcones on BmGST. Best docked poses are represented in figures (a) SK1, (b) SK2, (c) SK3, (d) SK4 (e) SK5, (f) SK6 and (g) SK7. Residues and ligands are shown in wireframe and stick form respectively. Colored according to the atoms—gray: carbon, red: oxygen, blue: nitrogen and green: chlorine. For clarity purpose hydrogen is omitted in ligands. Predicted hydrogen bonds between residues and ligand are highlighted with green dash lines and residues are colored according to amino acid type. Binding site represented with ribbon structure (red) wherever required.

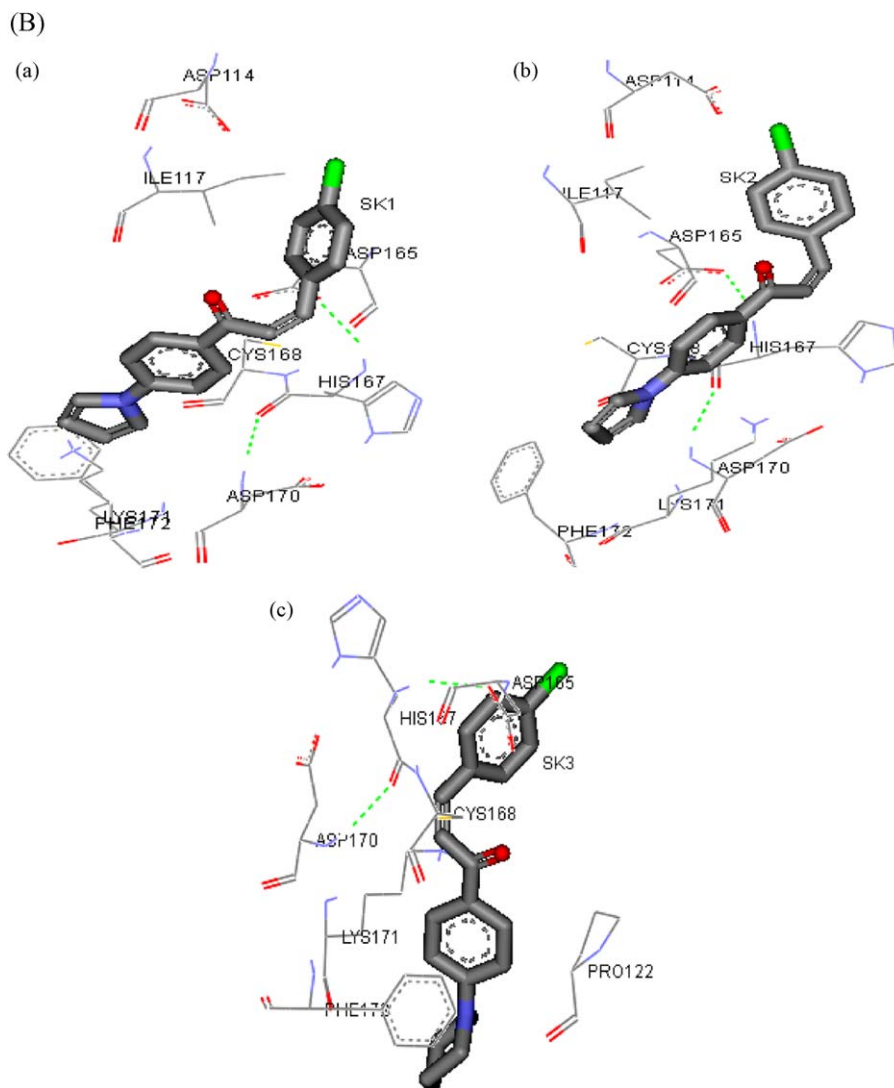


Fig. 4. (Continued)

experimental data where we have shown the significant inhibition of *Setaria cervi* GST by SK7 and proposed it as a potential antifilarial [13].

The chloro-substituted chalcones SK1, SK2 and SK3 were accommodated almost in equal manner in hydrophilic residues rich site located between  $\alpha$  5 and  $\alpha$  7 helices (Fig. 4Ba–Bc). The binding of these compounds leads to disruption of H-bonding between Asp114:Ile117 and formation of a new H-bond between His167 and Asp165 (data not shown). The angular dislocation in later two residues was clearly appeared to be linked with fitting of the ligand in binding pocket. However, because of located at far distance from ligand, the disruption of Asp114:Ile117 H-bond could not lead to any major changes in conformation and ligand binding.

In methyl-substituted chalcones, the binding location was observed in a crevice between  $\alpha$  1,  $\alpha$  6 and  $\alpha$  8. H-bonding was observed only in SK4 and SK5 binding (Table 4) while SK6 and SK7 accommodated through van der Waals force with protein receptor. As shown in Table 4 the H-bonding was found to be energetically stronger in SK5 with low formation energy compared to SK4 exhibiting the high affinity of SK5 to protein. This could be due to the involvement of O–H–N atoms between SK5 and residues.

Although both O–H–N (observed in SK5) and N–H–N (observed in SK4) are strong H-bonds still due to the opposite polarity in former one bonding was energetically stronger in SK5. The dissociation of H-bond between residues was also observed in methyl-substituted chalcones. Gln162:Asp159 interaction was most common in all four methyl-substituted chalcones binding site which were disrupted during docking and moved angularly for the proper adjustment of the ligand. While in the case of SK4, Gln208 dissociated its H-bond with Tyr109 to form a new H-bond with this ligand (data not shown). It appears that the disruption of H-bond between residues is not always associated with ligand accommodation but also with ligand interaction in order to achieve lowest energy orientation.

Noticeably, when GSH was docked in the presence of chloro and methyl-substituted chalcones similar observation as of Alb was noticed (Supplementary material). GSH could not bind with Tyr7 and docked at different locations. The change in the binding location of GSH with GST in the presence of chalcones supports our earlier report where chalcones were shown to inhibit GST activity by either forming Michael addition complex with GSH [13] or directly interacting with enzyme to lead conformational changes in enzyme active site.



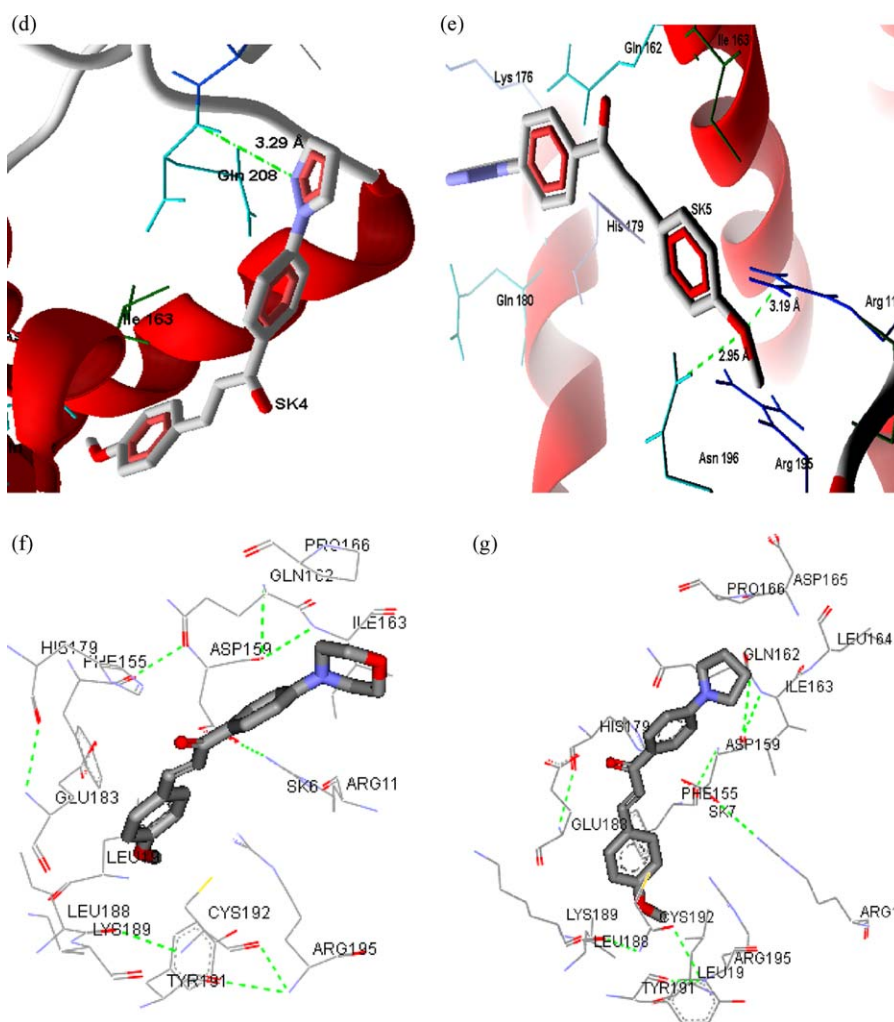


Fig. 4. (Continued).

#### 4. Conclusion

The observed difference in binding modes of various compounds with BmGST was firmly associated with their varied chemical structure. The combination of binding energy and hydrogen bonding interaction data suggests that Arg11, Ile163, His167 and Cys168 are most favorable common sites for antilhelmintics and chalcones binding (Fig. 5). The organic compounds used in the study interacted mainly through van der Waals forces and hydrogen bonds with protein receptor as described earlier [33]. We observed a potential interaction of nitro and oxy group of chalcones (SK4–7) and albendazole with BmGST structure. From the overall docking pattern of GSH and ligands we could propose that the binding of chalcones and albendazole (Fig. 6) change the protein conformation in such a manner that either narrow down the active site or widen to make it unfit for substrate binding. Besides, the large size of above compounds could also produce steric hindrances. The displacement of GSH from its original binding site due to ligand binding suggests a non-competitive type of inhibition in GST activity. This is the first report defining the structural information of BmGST and direct molecular interaction of available antilhelmintics with this model. We also proposed BmGST as potential template for drug targeting against filariasis. Additionally, using structural data of BmGST, screening and development of compounds could be evaluated for SAR studies. However, further investigation of the interaction mechanism of

these drugs with GST can be corroborated with experimental exposures. As explained by Marechal et al. [34] that both in silico and experimental methods complement each other in such a manner that could reduce long term trials and practical

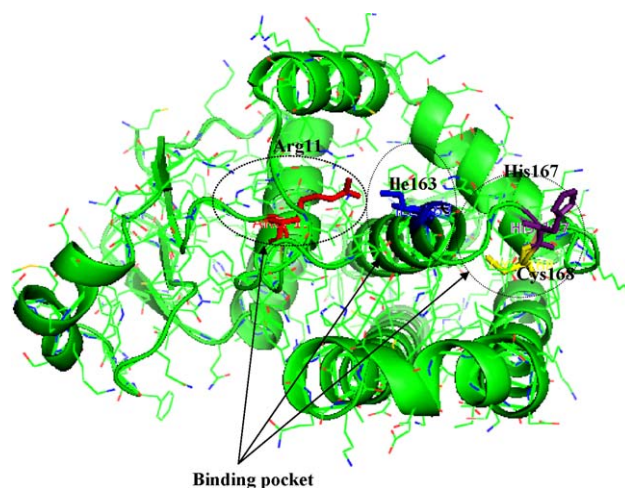
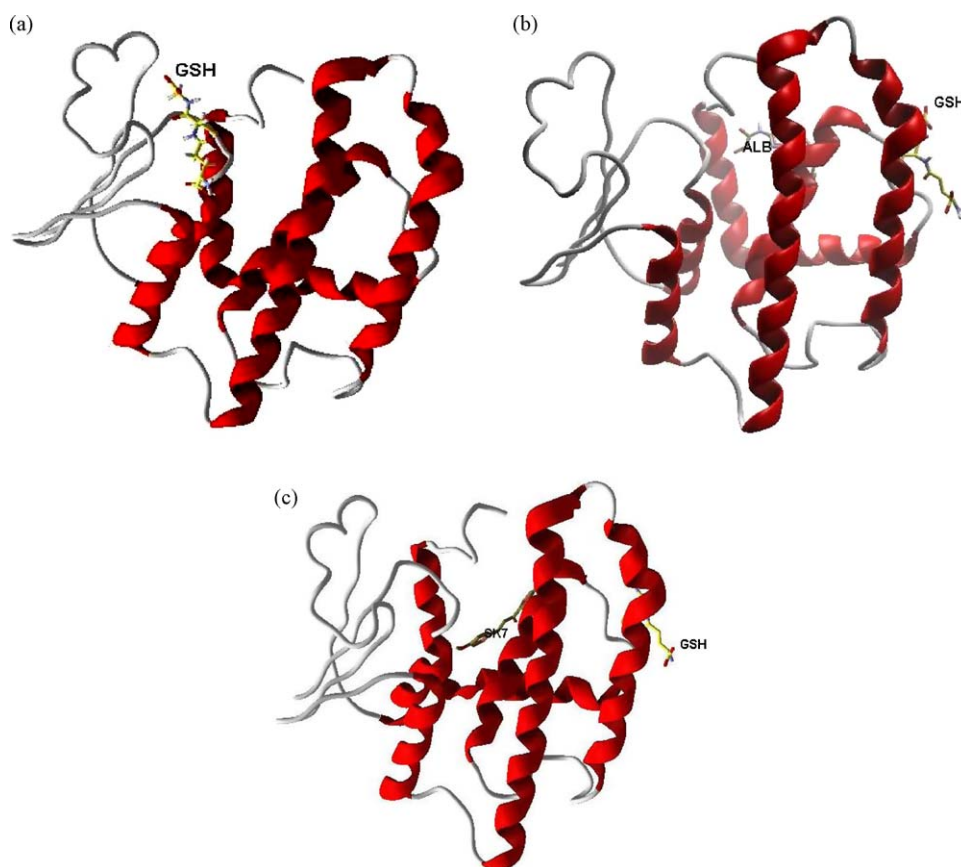


Fig. 5. Binding pockets formed by major residues: Arg11, Ile163, His167 and Cys168 are represented with red, blue, violet and yellow, respectively, on protein (GST) surface. Figure was drawn with PyMOL.



**Fig. 6.** (a–c) Binding mode of GSH in the presence of albendazole and a methyl-substituted chalcone SK7 on GST. For clarity, protein structure is represented in ribbon form;  $\alpha$  helices are shown as red ribbon while  $\beta$  sheets in gray tubes. GSH and drug ligands are shown as stick and colored according to carbon atoms. Figures were drawn with Molecular virtual viewer.

difficulties in drug targeting studies. Hence, it could be proposed that compounds having similar parent structure/backbone with modified functional groups could modulate the biological activity of protein in similar manner and considered to be better candidate as antifilarial agents.

### Conflict of interest

Authors state no conflict of interest.

### Acknowledgement

Authors are grateful to the University Grant Commission (MY) and Council of Scientific and Industrial Research scheme no. 37(1189)/04/EMR-II (SR) New Delhi, India for financial assistance.

### Appendix A. Supplementary data

Supplementary data associated with this article can be found, in the online version, at [doi:10.1016/j.jmglm.2009.10.003](https://doi.org/10.1016/j.jmglm.2009.10.003).

### References

- [1] D. Sheehan, G. Meade, V.M. Foley, C.A. Dowd, Structure, function and evolution of glutathione transferases: implications for classification of non-mammalian members of an ancient enzyme superfamily, *Biochem. J.* 360 (2001) 1–16.
- [2] M. Lefevre, K. Bourd, M.A. Loriot, M. Goldberg, P. Beaune, A. Périani, L. Stanislawski, TEGDMA modulates glutathione transferase P1 activity in gingival fibroblasts, *J. Dental Res.* 83 (12) (2004) 914–919.
- [3] P.M. Brophy, J. Barrett, Glutathione transferase in helminths, *Parasitology* 100 (1999) 345–349.
- [4] B. Mannervik, U.H. Danielson, Glutathione transferases, structure and catalytic activity, *CRC Crit. Rev. Biochem.* 23 (1998) 283–337.
- [5] M.P.C. Ibarra, M.L. Grillo, M. Belloc, T.K. Nucetellic, W.M. Atkinsa Bammler, Exploration of in vitro pro-drug activation and futile cycling by glutathione S-transferases: thiol ester hydrolysis and inhibitor maturation, *Arch. Biochem. Biophys.* 414 (2003) 303–311.
- [6] B.F. Coles, F.F. Kadlubar, Detoxification of electrophilic compounds by glutathione S-transferase catalysis: determinants of individual response to chemical carcinogens and chemotherapeutic drugs, *Biofactors* 17 (1–4) (2003) 115–130.
- [7] R.N. Armstrong, Structure, catalytic mechanism, and evolution of the glutathione-S-transferases, *Chem. Res. Toxicol.* 10 (1997) 2–18.
- [8] P.J. van Bladeren, Glutathione conjugation as a bioactivation reaction, *Chem. Biol. Interact.* 129 (2000) 61–76.
- [9] A. Torres-Rivera, A. Landa, Glutathione transferases from parasites: a biochemical view, *Acta Trop.* 105 (2008) 99–112.
- [10] D.L. Eaton, T.K. Bammler, Concise review on the glutathione S-transferases and their significance to toxicology, *Toxicol. Sci.* 49 (1999) 156–164.
- [11] W.Y. Precious, J. Barrett, The possible absence of cytochrome P-450 linked xenobiotic metabolism in helminths, *Biochim. Biophys. Acta* 992 (1989) 215–222.
- [12] S. Gupta, S. Rathaur, Filarial glutathione S-transferase: its induction by xenobiotics and potential as drug target, *Acta Biochim. Pol.* 52 (2) (2005) 7493–7500.
- [13] S.K. Awasthi, N. Mishra, S.K. Dixit, A. Singh, M. Yadav, S.S. Yadav, S. Rathaur, Antifilarial activity of 1,3-diarylpropen-1-one: effect on glutathione-S-transferase, a phase II detoxification enzyme, *Am. J. Trop. Med. Hyg.* 80 (5) (2009) 764–768.
- [14] T. Schwede, J. Kopp, N. Guex, M.C. Peitsch, SWISS-MODEL: an automated protein homology-modeling server, *Nucleic Acids Res.* 31 (2003) 3381–3385.
- [15] B.J. Mans, A.I. Louw, A.W.H. Neitz, The major tick salivary gland proteins and toxins from the soft tick, *Ornithodoros savignyi*, are part of the tick lipocalin family: implications for the origins of tick toxicoses, *Mol. Biol. Evol.* 20 (7) (2003) 1158–1167.
- [16] F. Melo, E. Feytmans, Assessing protein structures with a non-local atomic interaction energy, *J. Mol. Biol.* 277 (5) (1998) 1141–1152.
- [17] W.F. van Gunsteren, S.R. Billeter, et al., *Biomolecular Simulations: The GROMOS96 Manual and User Guide*, VdF Hochschulverlag ETHZ, Zürich, 1996.
- [18] V.N. Viswanadhan, A.K. Ghose, G.R. Revankar, R.K. Robins, Atomic physicochemical parameters for three dimensional structure directed quantitative structure-activity relationships. 4. Additional parameters for hydrophobic and dispersive interactions and their application for an automated superposition of certain

- naturally occurring nucleoside antibiotics, *J. Chem. Inf. Comput. Sci.* 29 (1989) 163–172.
- [19] D.W. Ritchie, Evaluation of Protein Docking Predictions using Hex 3.1 in CAPRI rounds 1–2, *Proteins: Struct. Funct. Genet.* 52 (2003) 98–106.
- [20] D.W. Ritchie, G.J.L. Kemp, Protein docking using spherical polar Fourier correlations, *Proteins: Struct. Funct. Genet.* 39 (2000) 178–194.
- [21] P. Daisy, S. Mathew, S. Suveena, N.A. Rayan, A novel terpenoid from *Elephantopus scaber* – antibacterial activity on *Staphylococcus aureus*: a substantiate computational approach, *Int. J. Biomed. Sci.* 4 (3) (2008) 3196–3203.
- [22] D.B.M. Virupakshaiah, K. Chandrakanth, P. Rachanagouda, H. Prasad, Computer aided docking studies on antiviral drugs for SARS, *World Acad. Sci. Eng. Technol.* 30 (2007) 297–299.
- [23] C. Hetenyi, D. van der Spoel, Blind docking of drug-sized compounds to proteins with up to a thousand residues, *FEBS Lett.* 580 (2006) 1447–1450.
- [24] S.T. Nathan, N. Mathew, M. Kalyanasundaram, K. Balaraman, Structure of glutathione S-transferase of the filarial parasite *Wuchereria bancrofti*: a target for drug development against adult worm, *J. Mol. Mod.* 11 (2005) 194–199.
- [25] D.G. Levitt, L.J. Banaszak, POCKET: a computer graphics method for identifying and displaying protein cavities and their surrounding amino acids, *J. Mol. Graph.* 10 (1992) 229–234.
- [26] M. Perbandt, J. Höppner, C. Betzel, R.D. Walter, E. Liebau, Structure of the major cytosolic glutathione S-transferase from the parasitic nematode *Onchocerca volvulus*, *J. Biol. Chem.* 280 (13) (2005) 12630–12636.
- [27] M. Wilce, M. Parker, Structure and function of glutathione S-transferases, *Biochem. Biophys. Acta* 1205 (1994) 1–18.
- [28] A. Parraga, I. Garciasae, S.B. WALSH, T.J. Mantle, M. Coll, The three-dimensional structure of a class- $\pi$  glutathione S-transferase complexed with glutathione: the active-site hydration provides insights into the reaction mechanism, *Biochem. J.* 333 (1998) 811–816.
- [29] W.L. DeLano, The PyMOL Molecular Graphics System, 2002 <http://www.pymol.org>.
- [30] P. Reinemer, H.W. Dirr, R. Ladenstein, J. Schaeffer, O. Gallay, R. Huber, The three-dimensional structure of class  $\pi$  glutathione S-transferase in complex with glutathione sulfonate at 2.3 Å resolutions, *EMBO J.* 10 (1991) 1997–2005.
- [31] S. Wolfa, M. Bockmanna, U. Howeler, J. Schlitter, K. Gerwerta, Simulations of a G protein-coupled receptor homology model predict dynamic features and a ligand binding site, *FEBS Lett.* 582 (2008) 3335–3342.
- [32] C.A. Lipinski, F. Lombardo, B.W. Dominy, P.J. Feeney, Experimental and computational approaches to estimate solubility and permeability in drug discovery and development settings, *Adv. Drug Deliv. Rev.* 23 (1–3) (1997) 3–25.
- [33] K. Chen, L. Kurgan, Investigation of atomic level patterns in protein–small ligand interactions, *PLoS One* 4 (2) (2009) 4473–4486.
- [34] J.D. Marechal, C.A. Kemp, G.C.K. Roberts, M.J.I. Paine, C.R. Wolf, Sutcliffe, Insights into drug metabolism by cytochromes P450 from modelling studies of CYP2D6–drug interactions, *Brit. J. Pharmacol.* 153 (2008) S82–S89.